



Structural, electronic, and magnetic properties of a series of aluminum clusters doped with various transition metals

Mei Wang^{a,b}, Xiaowei Huang^a, Zuliang Du^a, Yuncai Li^{a,*}

^a Key Laboratory for Special Functional Materials, Ministry of Education, Henan University, Kaifeng 475001, People's Republic of China

^b Department of Physics, Qufu Normal University, Qufu 273165, People's Republic of China

ARTICLE INFO

Article history:

Received 9 June 2009

In final form 9 September 2009

Available online 12 September 2009

ABSTRACT

The geometries, stabilities, and electronic and magnetic properties of MAI_n ($M = \text{Cr, Mn, Fe, Co, Ni}$; $n = 1-7, 12$) clusters have been investigated systematically within the framework of the gradient-corrected density-functional theory. MAI_n clusters have similar geometries as that of Al_{n+1} clusters. For MAI_{12} clusters, only cobalt and the nickel atoms, whose atom radius are smaller, prefer a position at the cluster center of icosahedron. MAI_3 clusters possess relatively higher stability. All the HOMO and LUMO states are non-degenerate and delocalized. The computed total magnetic moments of the lowest-energy structures oscillate with the cluster size, and NPA shows that the 3d electrons play a dominant role for the magnetism of the system.

© 2009 Published by Elsevier B.V.

1. Introduction

During the last two decades numerous theoretical and experimental efforts have been devoted to studying the structural, electronic, optical and magnetic properties of atomic clusters [1–5]. The properties of atomic clusters are distinctly different from those of bulk materials, and they change drastically with increasing cluster size. Therefore, studying the structure of amorphous systems in relation to the cluster size is a prerequisite for understanding their special physical and chemical properties.

As a typical example of atomic clusters, aluminum cluster has been a subject of many theoretical and experimental studies [6–10]. And a lot of computational investigations have been conducted on pure aluminum clusters. For example, Yang et al. [11] have reported *ab initio* molecular-dynamics simulation of small aluminum clusters Al_n ($n = 2-6$, and 12, 13, 55 and 147) by using density-functional and Sankey local-orbital method. Cohen et al. have found that the stability of small Al_n clusters can be explained using jellium model, because the valence electrons of Al have free-electron-like behavior [12,13]. Recently, much attention has been paid to doped aluminum clusters. And many types of elements such as nonmetals (H, B, C, P, S, N) [9,14–18], reactive metals (Na, Mg) [19,20], and transition metals (Ti, Fe, Ni) [21–23] have been tried as substitutes to search stabilized doped aluminum clusters. Among various doped Al clusters, those doped with transition metals (TM) have been increasingly focused on. This is largely because single transition metal element isolated in a *sp* metal host is an ideal classical system for studying how the *d* electron interacts with the nearly free electron gas forming a local

magnetic moment. Also it is because transition metal elements can display unusually large local magnetic moments when they are absorbed on or embedded into the *sp* metal surface. Ni–Al clusters, for example, are the subject of several previous theoretical and experimental studies and have been accepted as useful models for investigating the key factors responsible for the atomic ordering or segregation in nanoalloy clusters [24–26]. Unfortunately, the research on the magnetic properties of small Ni–Al clusters virtually remains vacant but for the interesting progression, established by Reddy et al. [22], about the magnetic behavior of very small $(\text{FeAl})_n$ ($n \leq 6$) clusters and bulk FeAl.

Therefore, our interest is placed on the structural and electronic as well as magnetic properties of TM-doped Al clusters in the present research, and spin-density-functional calculations are done for a wide range of 3d dopant atoms and MAI_n ($M = \text{Cr, Mn, Fe, Co, Ni}$; $n = 1-7, 12$) clusters. Hopefully, the calculations are to shed light on how magnetic properties change as the local electrons of an isolated atom begin to delocalize in MAI_n clusters and how the magnetism of MAI_n clusters varies with increasing cluster size. Thus the computational details are briefed in Section 2. The lowest-energy structures of MAI_n ($M = \text{Cr, Mn, Fe, Co, Ni}$) clusters and their growth behavior, together with the electronic and magnetic properties of the clusters, are discussed in Section 3. And conclusions are finally given in Section 4.

2. Theoretical methods

All calculations are performed using density-functional theory (DFT) provided in the DMOL3 package [27]. Since the reliability of DFT studies depends on the choice of the functional and the basis set for the problem under investigation, the density-functional calculations are done by treating the exchange–correlation interaction

* Corresponding author. Fax: +86 378 3886375.

E-mail address: liyuncaihenu.edu.cn (Y. Li).

with generalized gradient approximation (GGA) using Perdew–Wang 1991 (PW91) functional [28]. All electron treatment and double numerical basis including with polarized (DNP) functions are chosen. Self-consistent field calculations are done with a convergence criterion of Hartree on total energy scale. The density mixing criteria for charge and spin are 0.02 and 0.05, respectively. Since natural orbital population analysis (NPA) is carried out on the ground-state structures, and NPA computation is unavailable in the DMOL package, the PW91 functional and the LANL2DZ basis set implemented in the GAUSSIAN-03 package are used for computations in our present research [29,30].

To benchmark the modeling elements of the computational method employed in this study, calculations are done for Al₂ and FeAl dimers in the first stage, due to the availability of their experimental and theoretical data for comparison. The bond length, average binding energy, and vibrational frequency of Al₂ are calculated to be 2.601 Å, 0.908 eV, and 319.7 cm⁻¹, respectively, agreeing well with the experimental values of 2.560 Å, 0.997 ± 0.108 eV, and 350.01 cm⁻¹ [31]. And the bond length, binding energy, and multiplicity of FeAl are calculated to be 2.424 Å, 3.102 eV, and 4, respectively, well conforming to the DFT results (2.43 Å, 3.29 eV, and 4) reported by Reddy et al. [22]. This indicates it is efficient and reliable to use the same basis set for the DFT calculations of small MAI_n clusters.

The number of distinct initial geometries is important to the reliability of the ground-state structures obtained. In order to obtain the lowest-energy structures of MAI_n clusters, different spin multiplicities and a considerable amount of possible initial structures are considered for each size. We obtained the specific initial structures by several ways as follows: (1) Using the same method, we firstly optimized the equilibrium geometries of Al_n clusters. On the basis of the optimized Al_n geometries, we considered possible isomeric structures by placing the M atom on each possible site of Al_n cluster as well as by substituting one Al atom in Al_{n+1} cluster with one M atom, using previous studies of chromium, manganese, iron, cobalt, and nickel clusters as the guide. (2) In general, clusters with higher symmetry and fewer surface atoms are expected to be more stable. Therefore, according to a certain symmetry, the initial geometry is constructed. Especially, the Jahn–Teller theory is employed to search for the ground-state structure. (3) The energetically most favorable geometries of other transition-metal-doped aluminum clusters previously published in literatures are also taken as the guidance. The number of structural candidates depends on the size of cluster. For example, four kinds of initial configuration are considered for MAI₃, while the number of structural isomers increases to 30 for MAI₇. Overall, more than 200 kinds of configuration are considered to ensure that our results are reliable. For a given initial structure, spin-unrestricted calculations are performed for all allowable spin multiplicities. Starting with the spin singlet configuration of even-electron systems and the spin doublet configuration of odd-electron systems, the calculations are implemented until the minimum energy is reached. The harmonic vibration frequencies are also calculated so as to verify the nature of the stationary point on potential energy surfaces. If an imaginary vibrational mode is found, a relaxation along the coordinates of this mode is carried out until the true local minimum is actually obtained. Therefore, all isomers for each cluster are surely corresponding to the local minima.

3. Results and discussion

3.1. Equilibrium geometries

The lowest-energy structures of Al_{n+1} and MAI_n (*n* = 1–7, 12; M = Cr, Mn, Fe, Co, Ni) clusters calculated using the computation

scheme described in Section 2 are presented in Fig. 1. At the same time, the symmetry, spin multiplicity, binding energy, HOMO–LUMO (highest occupied molecular orbital–lowest unoccupied molecular orbital) gap, and charge of M atom for the lowest-energy structures of MAI_n clusters are listed in Table 1. Calculations in the present research indicate that the spin multiplicities of MAI_n (*n* = 1–7, 12; M = Cr, Mn, Fe, Co, Ni) clusters follow the sequences 6, 5, 4, 1, 6, 5, 4, 5; 5, 4, 3, 2, 1, 2, 3, 6; 4, 3, 2, 3, 4, 5, 2, 7; 3, 2, 1, 2, 1, 4, 1, 2; and 2, 1, 2, 3, 2, 3, 2, 3, respectively. Moreover, as shown in Fig. 1, the equilibrium structures of Al_n clusters (*n* = 2–4) are all of planar geometries which can be obtained by adding one Al atom to one side of the Al_{n-1} structures. This is in good agreement with previous theoretical work [11].

For MAI₂ (M = Cr, Mn, Fe, Co, Ni) clusters, the geometry in the lowest energy state is an isosceles triangle (C_{2v}), and the average distance of M–Al bond reduces gradually in an order of Cr, Mn, Fe, Co, and Ni. Likewise, the binding energy of the lowest energy state of MAI₂ clusters increases gradually in the same order. MAI₃ clusters are the smallest clusters that display a three-dimen-

Table 1

The symmetry *S*, spin multiplicity 'Multi', binding energy per atom *E_b* (eV), HOMO–LUMO gap *E_g* (eV), and charge *Q* (e) of the M atom in the lowest-energy structures of MAI_n clusters.

Cluster	<i>S</i>	Multi	<i>E_b</i>	<i>E_g</i>	<i>Q</i>
Al ₂	<i>D_{∞h}</i>	3	0.908	0.350	
Al ₃	<i>D_{3h}</i>	2	1.445	0.527	
Al ₄	<i>D_{2h}</i>	1	1.635	0.105	
Al ₅	<i>C₂</i>	2	1.862	0.008	
Al ₆	<i>D_{3d}</i>	1	2.133	0.673	
Al ₇	<i>C_{3v}</i>	2	2.343	0.815	
Al ₈	<i>D_{2d}</i>	3	2.337	0.617	
Al ₁₃	<i>I_h</i>	2	2.679	1.890	
CrAl	<i>C_{∞v}</i>	6	0.684	0.875	0.108
CrAl ₂	<i>C_{2v}</i>	5	1.272	0.449	0.254
CrAl ₃	<i>C_{3v}</i>	4	1.668	0.628	0.267
CrAl ₄	<i>C_{4v}</i>	1	1.729	0.563	-0.569
CrAl ₅	<i>C_s</i>	6	1.971	0.652	0.493
CrAl ₆	<i>C_s</i>	5	2.198	0.306	0.489
CrAl ₇	<i>C₁</i>	4	2.307	0.537	0.490
CrAl ₁₂	<i>C_s</i>	5	2.576	0.300	0.538
MnAl	<i>C_{∞v}</i>	5	0.800	0.405	0.025
MnAl ₂	<i>C_{2v}</i>	4	1.487	1.005	0.244
MnAl ₃	<i>C_{3v}</i>	3	1.807	1.107	0.154
MnAl ₄	<i>C_{4v}</i>	2	1.929	0.851	0.289
MnAl ₅	<i>C_s</i>	1	2.088	1.260	0.101
MnAl ₆	<i>C_{2v}</i>	2	2.203	0.329	0.311
MnAl ₇	<i>C₁</i>	3	2.358	0.626	0.350
MnAl ₁₂	<i>C_s</i>	6	2.626	0.249	0.860
FeAl	<i>C_{∞v}</i>	4	1.551	0.951	-0.116
FeAl ₂	<i>C_{2v}</i>	3	1.943	0.767	-0.010
FeAl ₃	<i>C_{3v}</i>	2	2.222	0.925	-0.113
FeAl ₄	<i>C_{4v}</i>	3	2.284	0.353	-0.046
FeAl ₅	<i>C₁</i>	4	2.306	0.489	-0.071
FeAl ₆	<i>C_{2v}</i>	5	2.474	0.486	0.267
FeAl ₇	<i>C_s</i>	2	2.583	0.725	0.137
FeAl ₁₂	<i>C_{5v}</i>	7	2.722	0.389	0.506
CoAl	<i>C_{∞v}</i>	3	2.131	1.263	-0.157
CoAl ₂	<i>C_{2v}</i>	2	2.366	1.242	-0.154
CoAl ₃	<i>C_{3v}</i>	1	2.636	1.608	-0.439
CoAl ₄	<i>C_{4v}</i>	2	2.555	0.210	-0.243
CoAl ₅	<i>C_s</i>	1	2.553	0.737	-0.209
CoAl ₆	<i>C₂</i>	4	2.625	0.637	-0.229
CoAl ₇	<i>C₁</i>	1	2.735	0.763	-0.289
CoAl ₁₂	<i>D_{3d}</i>	2	2.833	0.493	-0.659
NiAl	<i>C_{∞v}</i>	2	2.254	0.330	-0.237
NiAl ₂	<i>C_{2v}</i>	1	2.570	0.602	-0.138
NiAl ₃	<i>C_{3v}</i>	2	2.684	1.177	-0.123
NiAl ₄	<i>C_{4v}</i>	3	2.613	0.589	-0.102
NiAl ₅	<i>C_s</i>	2	2.590	0.502	-0.022
NiAl ₆	<i>C_{3v}</i>	3	2.683	0.440	0.095
NiAl ₇	<i>C_s</i>	2	2.800	0.579	-0.007
NiAl ₁₂	<i>I_h</i>	3	2.898	0.320	-0.273

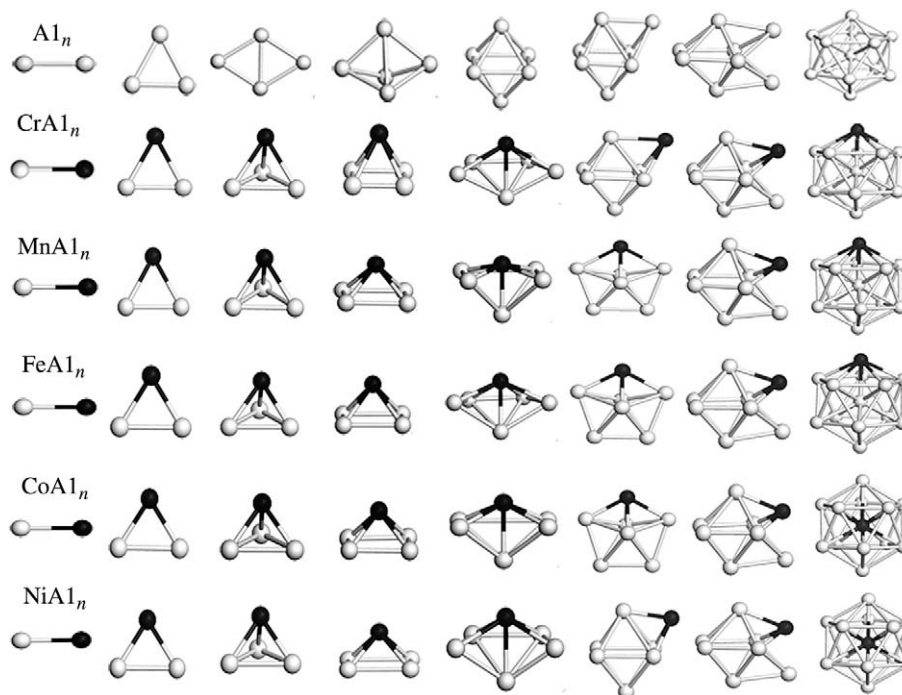


Fig. 1. Equilibrium geometries of Al_{n+1} and MAI_n clusters. The gray and black balls represent Al and M atoms, respectively.

sional structure. Three Al atoms form an equilateral triangle and the M atom caps the surface resulting in a tetrahedral configuration. All the MAI_3 clusters under investigation have a C_{3v} symmetry. This observation is different from previous DFT calculations for Au_nM^+ ($M = Sc, Ti, V, Cr, Mn, Fe, Au; n = 1-9$) [32] and MB_n ($M = Cr, Mn, Fe, Co, Ni; n = 1-7$) [33] clusters, which also show that the 3D geometries begin at $n = 7$. For MAI_4 , the ground-state structure is a square pyramidal arrangement (C_{4v}), which can be obtained by adsorbing one additional M atom on the face center of the square unit. For MAI_5 clusters, a lot of possible structural configuration and spin states have been tried to identify the ground state. As a result, the octahedron, capped trigonal bipyramid, pentagonal pyramid, and triangular prism with different symmetries are optimized. And a distorted Al capped trigonal bipyramid with M atom at the triangular ring is obtained as the lowest-energy structure for MAI_5 with a symmetry of C_s except for $FeAl_5$ (C_1). For MAI_6 , the isomers such as capped octahedron, bicapped hexahedron, pentagonal bipyramid, and capped prism are considered as initial geometries. The lowest-energy structure for $CrAl_6$ and $NiAl_6$ can be referred to as Al_7 cluster which is mono-substituted by one Cr or Ni atom. And the pentagonal bipyramid is the lowest-energy configuration for $MnAl_6$, $FeAl_6$, and $CoAl_6$. Moreover, among various isomers of MAI_7 , the ground-state structures are adjacent bicapped octahedrons with C_1 ($M = Cr, Mn, Co$) and C_s ($M = Fe, Ni$) symmetry.

For MAI_{12} clusters, we have considered all different sites for one M atom in the configurations including icosahedron, cuboctahedron, and decahedron. And the lowest-energy structures of the MAI_{12} clusters are determined to be icosahedrons. At the same time, the atom of M, as a substitution of single Al atom, prefers residing at the surface in $CrAl_{12}$, $MnAl_{12}$, and $CoAl_{12}$ clusters, similar as in XAl_{12} ($X = Cu, Ag, Au, Ge, Sn, Pb$) clusters [34,35]. However, $CoAl_{12}$ and $NiAl_{12}$ have stable icosahedron structures whose impurity atom inhabits the center. Usually, due to the strong tendency of the bulk alloy to form ordered compounds, M atom may prefer to reside at the center of doped aluminum clusters, leading to increased number of M–Al bonds. However, if a large M atom (e.g.,

Cr, Mn, and Fe) is placed at the center of the icosahedron, the MAI_{12} clusters will undergo a slight expansion leading to increased energy of the Al–Al bonds. Such an increase of the energy of Al–Al bonds in MAI_{12} clusters caused by central dopant may be easily incurred, since the surface atoms of metallic systems tend to contract for the compensation of lowered coordination. Therefore, among various dopant atoms such as Cr, Mn, Fe, Co, Ni, Cu, Ag, Au, Ge, Sn, and Pb, only Co and Ni atoms with a radius smaller than that of Al atom prefer to reside at the center of MAI_{12} clusters.

3.2. Relative stabilities

In order to understand the relative stability and size-dependent behavior of MAI_n clusters, we have investigated the average binding energy per atom [$E_b(n)$], the fragmentation energy [$D(n, n-1)$], and the second-order differences of energies [Δ_2E]. Here the average binding energy, fragmentation energy, and second-order differences of energies for the MAI_n clusters are defined as:

$$E_b(n) = [E_T(M) + nE_T(Al) - E_T(MAl_n)]/n + 1$$

$$D(n, n-1) = E(MAl_{n-1}) + E(Al) - E(MAl_n)$$

$$\Delta_2E(n) = E(MAl_{n+1}) + E(Al_{n-1}M) - 2E(MAl_n)$$

Where $E(\dots)$ is the total energy of the corresponding system.

Fig. 2 shows the average binding energy of various MAI_n clusters. It is seen that the average binding energy of MAI_n ($M = Cr, Mn, Fe$) increases with increasing cluster size, and it seems that the average binding energy of $CoAl_n$ and $NiAl_n$ clusters is of a larger fluctuation. At the same time, $CrAl_n$ and $MnAl_n$ clusters, excluding CrB_3 , $MnAl_2$, $MnAl_3$, and $MnAl_4$, have lower binding energies than pure Al_n . This indicates that doping Cr atom leads to decrease of the stability of Al_n clusters, while doping Mn, Fe, Co, and Ni atoms improves the stability of Al_n clusters. Besides, a local binding energy peak appears at $n = 3$, implying that MAI_3 clusters are more stable than their neighboring clusters.

Fig. 3 shows the fragmentation energy and second-order differences of total energies of MAI_n clusters. The local abundant peaks

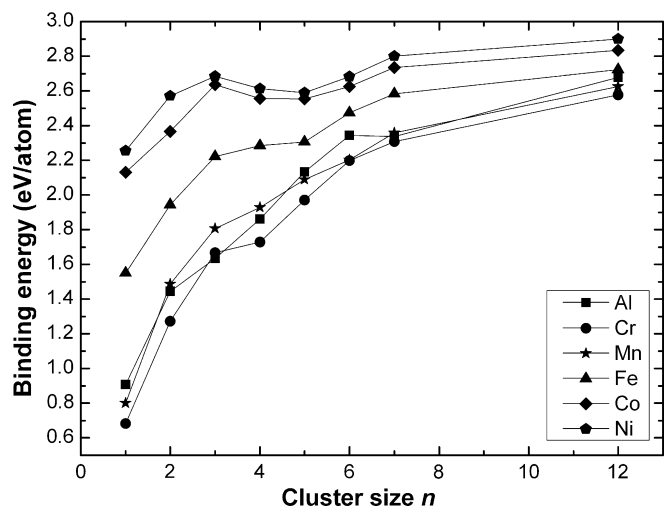


Fig. 2. Size-dependence of the average binding energy of Al_{n+1} and MAI_n clusters.

of $D(n, n-1)$ appear at $n=3$, and the maxima of second-order differences of energies also emerge at $n=3$ for the same systems. This, the same as what has been observed for average binding energy, also means that MAI_3 clusters possess higher stability than their neighbors.

The HOMO–LUMO gap is a characteristic quantity of electronic structure of clusters and also a measure of the ability for clusters to undergo activated chemical reactions with small molecules. Shown

in the right panels of Fig. 3 is the difference between the eigenvalues of the LUMO and HOMO for various MAI_n clusters. The same as that observed for $E_b(n)$ and Δ_2E , the HOMO–LUMO gap of various MAI_n clusters reaches a maximum also at $n=3$, corresponding to stronger chemical stability of MAI_3 clusters than their neighbors. Moreover, as shown in Table 1, MAI_{12} ($M = Cr, Mn, Fe, Co, Ni$) clusters have smaller HOMO–LUMO gaps than Al_{13} , the same as $TiAl_{12}$ with a small HOMO–LUMO gap but contrary to XAl_{12} ($X = B, C, Si, Ge$) with large HOMO–LUMO gaps [21]. This might be attributed to the strong interaction between the $3d$ orbitals and other electronic orbitals of the transition metals as compared with B, C, Si, Ge.

To investigate the bonding nature of various MAI_n clusters in relation to molecular orbitals, we have examined the partial density of states in terms of the contribution of different orbital components (s, p, d) and the electron density of the HOMO and LUMO states. Detailed analyses of electronic levels show that the HOMO and LUMO of various MAI_n clusters mainly consist of $3d, 4s$, and $4p$ states of transition metal M mixed with $3s$ and $3p$ states of Al. The distribution of electron density of HOMO and LUMO states of some MAI_n clusters is shown in Fig. 4. It is seen that all the HOMO and LUMO states are non-degenerate and show delocalized behavior. Therefore, the change of HOMO–LUMO gap caused by doping M atom should be attributed to the hybrid states. In addition, as seen in Fig. 4, the d orbital's hybridization intensity of M (Cr, Mn, Fe, Co, Ni) with the orbital of Al reduces gradually. Namely, there is a strong hybridization between the s and d orbitals of Cr and the s and p orbitals of Al in $CrAl_n$, but the d orbitals of Co and Ni are only weakly hybridized with the orbital of Al in $CoAl_n$ and $NiAl_n$. The reason might lie in that the electron affinity and the

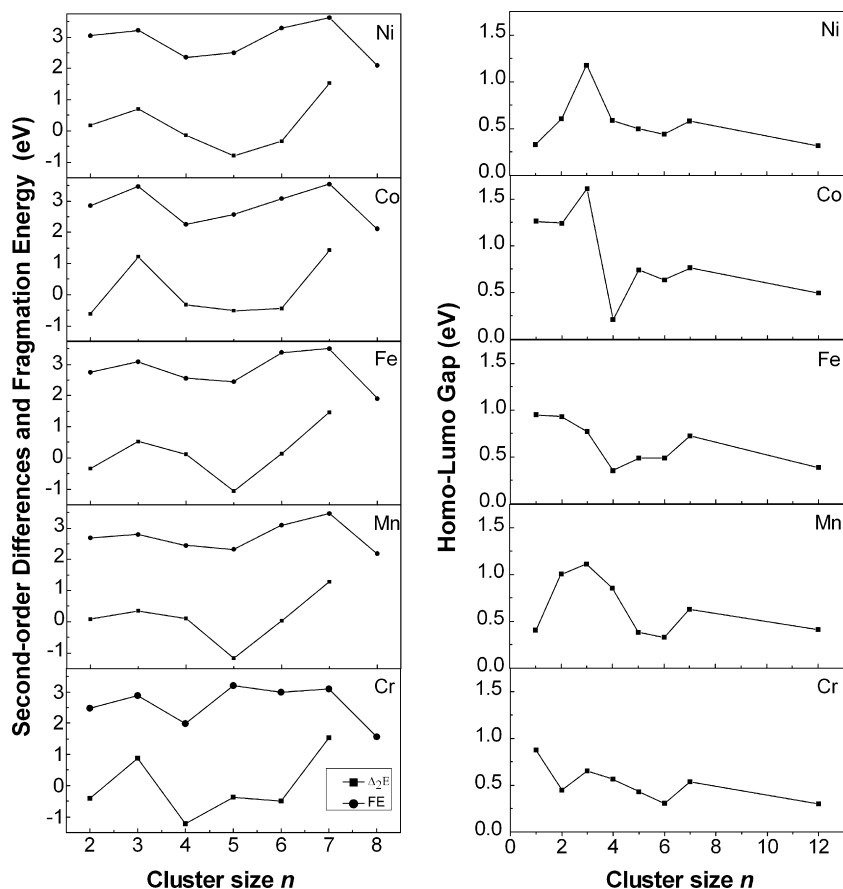


Fig. 3. Left panels: Size dependence of the fragmentation energy and second-order energy differences of MAI_n clusters; Right panels: Size dependence of the HOMO–LUMO gaps of MAI_n clusters.

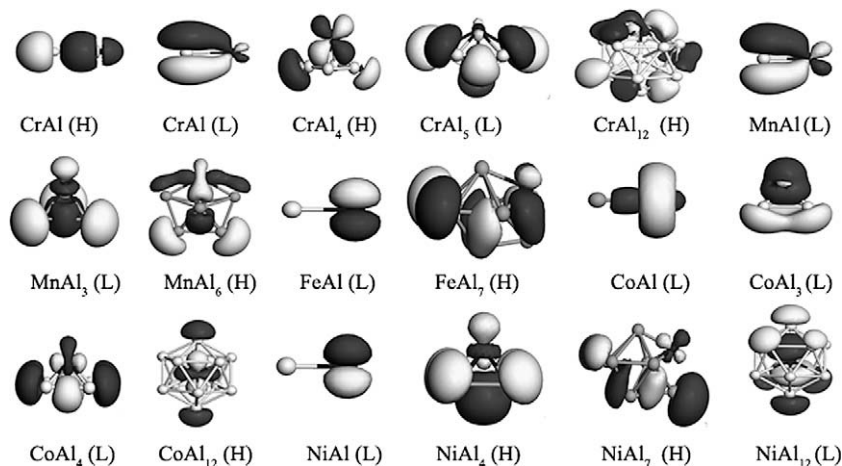


Fig. 4. The HOMO and LUMO orbitals of MAI_n clusters.

number of $3d$ electron pair increase gradually in an order of Cr, Mn, Fe, Co, and Ni, leading to increasingly weaker d orbital's hybridization intensity.

3.3. Magnetic moment

In order to gain more insights into the magnetic nature of MAI_n clusters, we have also implemented a detailed analysis on the on-site atomic charges and local magnetic moments of M atom, and the results are presented in Table 2. The local magnetic moment of various transition metals decreases gradually following an order of Cr, Mn, Fe, Co, and Ni, conforming to the gradual reduce of their number of unpaired d electrons. For $CrAl_n$, $MnAl_n$ and $FeAl_n$ clusters, the total magnetic moment is mainly located on M atom, and most of the local magnetic moments on Al atoms of those clusters, excluding $CrAl_5$, $MnAl_{12}$, $FeAl_5$, $FeAl_6$ and $FeAl_{12}$ with a ferromagnetic alignment, are aligned antiferromagnetically, but the magnetic moment of Cr atom is quenched at $n = 4$. For $CoAl_n$ clusters, excluding $CoAl_{12}$, the total magnetic moment is mainly located on Co atom. The local magnetic moment of Co atom with even n , also excluding $CoAl_{12}$, approaches the bulk moment ($1.17\mu_B$), and that of Co atom with odd n , excluding $CoAl$, is quenched. For $NiAl_n$ clusters, the total magnetic moment as a function of the cluster size shows pronounced odd–even effects. Namely, $NiAl_n$ clusters with odd n all have a total magnetic moment of $2\mu_B$, while $NiAl_n$ clusters with even n , excluding $NiAl_2$, have a total magnetic moment of $1\mu_B$. Moreover, different from that observed in clusters $CrAl_n$, $MnAl_n$, $FeAl_n$, and CoB_n , a small magnetic moment is located on the Ni atom in $NiAl_n$ clusters, and most of the local moments on Al atoms are aligned ferromagnetically.

In terms of the magnetic moments of open $3d$ transition-metal-doped Al clusters, it is interesting to note some trends of the magnetic moments of MAI_n .

(1) The magnetic moments of MAI and MAI_2 clusters (Cr, Mn, Fe, Co, Ni), which are the planar structures, are 5, 4, 3, 2, $1\mu_B$ and 4, 3, 2, 1, $0\mu_B$, respectively. Their magnetic behavior can be interpreted in light of the valence-bond theory. Every Al atom needs to capture one electron from neighboring M atom forming covalent bond in the cluster. For $CrAl$, one $4s$ electron of Cr ($3d^5 4s^1$) atom tends to transfer to Al, leaving five $3d$ electrons, responsible for the net spins of $5\mu_B$. In accordance with the Hund's rule, the magnetic moments of Mn, Fe, Co, and Ni atoms are 5, 4, 3, $2\mu_B$, respectively. However, for MAI (Mn, Fe, Co, Ni), because two $4s$ electrons stay in filled shell, one $3d$ electron tends to transfer to Al. Therefore,

Table 2

The total magnetic moment $TM(\mu_B)$ and magnetic moment $M(\mu_B)$ of the M atom, and the charge $Q(e)$ and magnetic moment $M(\mu_B)$ of $3d$, $4s$, and $4p$ states for M atom in MAI_n clusters.

Cluster	M	TM	3d		4s		4p	
			Q	M	Q	M	Q	M
CrAl	5	5.191	4.88	4.721	1.19	1.178	0.03	0.069
CrAl ₂	4	4.860	4.91	4.488	0.82	0.369	0.02	0.005
CrAl ₃	3	4.484	4.95	4.172	0.65	0.244	0.02	0.171
CrAl ₄	0	0	5.92	0	0.60	0	0.05	0
CrAl ₅	5	4.550	4.99	4.190	0.46	0.189	0.06	0.174
CrAl ₆	4	4.674	4.96	4.349	0.53	0.261	0.02	0.067
CrAl ₇	3	4.526	4.98	4.223	0.50	0.215	0.03	0.091
CrAl ₁₂	4	4.236	4.92	3.847	0.47	0.233	0.06	0.160
MnAl	4	4.683	5.58	4.286	1.36	0.402	0.02	-0.004
MnAl ₂	3	4.325	5.72	4.024	0.99	0.307	0.03	-0.002
MnAl ₃	2	3.669	6.04	3.441	0.77	0.183	0.02	0.050
MnAl ₄	1	1.495	6.32	1.416	0.70	0.059	0.04	0.022
MnAl ₅	0	0	7.55	0	0.76	0	0.07	0
MnAl ₆	1	3.683	6.03	3.462	0.61	0.201	0.04	0.025
MnAl ₇	2	3.630	6.08	3.406	0.51	0.169	0.05	0.060
MnAl ₁₂	5	4.188	5.83	3.892	0.22	0.181	0.07	0.122
FeAl	3	3.461	6.71	3.175	1.38	0.291	0.01	-0.004
FeAl ₂	2	2.903	6.95	2.714	1.02	0.202	0.03	-0.011
FeAl ₃	1	2.204	7.28	2.072	0.79	0.112	0.04	0.023
FeAl ₄	2	2.217	7.28	2.134	0.71	0.080	0.04	0.007
FeAl ₅	3	2.369	7.35	2.214	0.62	0.082	0.08	0.075
FeAl ₆	4	2.944	6.98	2.701	0.67	0.176	0.07	0.071
FeAl ₇	1	2.557	7.26	2.407	0.53	0.124	0.07	0.030
FeAl ₁₂	6	3.408	6.96	3.010	0.43	0.301	0.08	0.102
CoAl	2	2.276	7.84	2.015	1.30	0.265	0.01	-0.002
CoAl ₂	1	1.588	8.13	1.454	0.98	0.140	0.02	-0.004
CoAl ₃	0	0	8.62	0	0.77	0	0.05	0
CoAl ₄	1	1.077	8.44	0.986	0.73	0.077	0.06	0.016
CoAl ₅	0	0	8.68	0	0.62	0	0.12	0
CoAl ₆	3	1.639	8.30	1.521	0.59	0.067	0.07	0.053
CoAl ₇	0	0	8.68	0	0.52	0	0.08	0
CoAl ₁₂	1	0.004	9.07	0.110	0.36	0.026	0.13	0.079
NiAl	1	1.116	8.87	1.076	1.35	0.043	0.01	-0.002
NiAl ₂	0	0	9.26	0	0.98	0	0.02	0
NiAl ₃	1	0.178	9.31	0.160	0.76	0.015	0.04	0.003
NiAl ₄	2	0.627	9.28	0.579	0.74	0.040	0.07	0.009
NiAl ₅	1	0.277	9.32	0.277	0.59	0.002	0.11	-0.002
NiAl ₆	2	0.585	9.22	0.540	0.63	0.036	0.05	0.010
NiAl ₇	1	0.073	9.38	0.071	0.54	0.152	0.09	0.042
NiAl ₁₂	2	0.101	9.52	0.094	0.39	0.042	0.26	0.152

their magnetic moments are 4, 3, 2, $1\mu_B$, respectively. The same situation happens to MAI_2 clusters.

(2) The magnetic moments of MAI_3 (C_{3v}) and MAI_4 (C_{4v}) clusters (Cr, Mn, Fe, Co, Ni), which are the three-dimensional structures, are

3, 2, 1, 0, $1\mu_B$, and 0, 1, 2, 1, $2\mu_B$, respectively. Their magnetic behavior can be interpreted in light of the spherical jellium model [12]. The valence electrons are sufficient to completely fill an electronic shell, e.g., $1s, 1p, 1d, \dots$ For CoAl_3 and CrAl_4 , they have eighteen electrons to form stable close-shell electronic structure, and thus the clusters have zero spin.

(3) For MAl_n ($n > 4$) clusters, their geometrical shape basically deviates from spherical structure, and the energy level should also change significantly. As an effort to explain this phenomenon of the magnetic moment in MAl_n ($n > 4$) clusters, we plot the partial densities of states (PDOS) of the clusters. Fig. 5 gives the PDOS of some MAl_n clusters (FeAl_5 and CoAl_7) as representatives. It can be clearly seen that the electronic states below Fermi level mainly come from d state and the contributions from s and p states are very little. $3d$ orbitals heavily interact with other electronic orbitals, and there is a strong spd hybridization. Similar behavior was observed for all the clusters with other size. As shown in Table 2, the charge transfer in MAl_n clusters mainly happens within the $4s, 3d$, and $4p$ states of M to $3s$ and $3p$ states of Al . There exists sd - p hybridization in M atom and s - p hybridization in Al atom.

Because there is some hybridization between the atomic orbitals of the guest atom M and host atom Al , the magnetic moment of M atom shows a large variation. Using NiAl_7 cluster as an example, the magnetic moment of Ni atom is reduced to only $0.073\mu_B$. For CoAl_7 cluster, symmetric spin is observed, indicating its zero magnetic moment.

4. Conclusions

In summary, we have studied the growth behavior, stability, and electronic and magnetic properties of MAl_n ($n = 1-7, 12$) clusters using DFT based on generalized gradient approximation. The resulting MAl_n clusters have similar geometries as that of Al_{n+1} clusters, where the M atom can be thought of as a substitutional impurity in the Al_{n+1} clusters with a slight distortion on the whole. For MAl_n clusters, substitutional atoms Cr, Mn , and Fe prefer to reside at the cluster surface, while Co and Ni dopant atoms prefer to reside at the cluster center. The stability analysis in relation to the calculation of the average binding energy and second-order energy

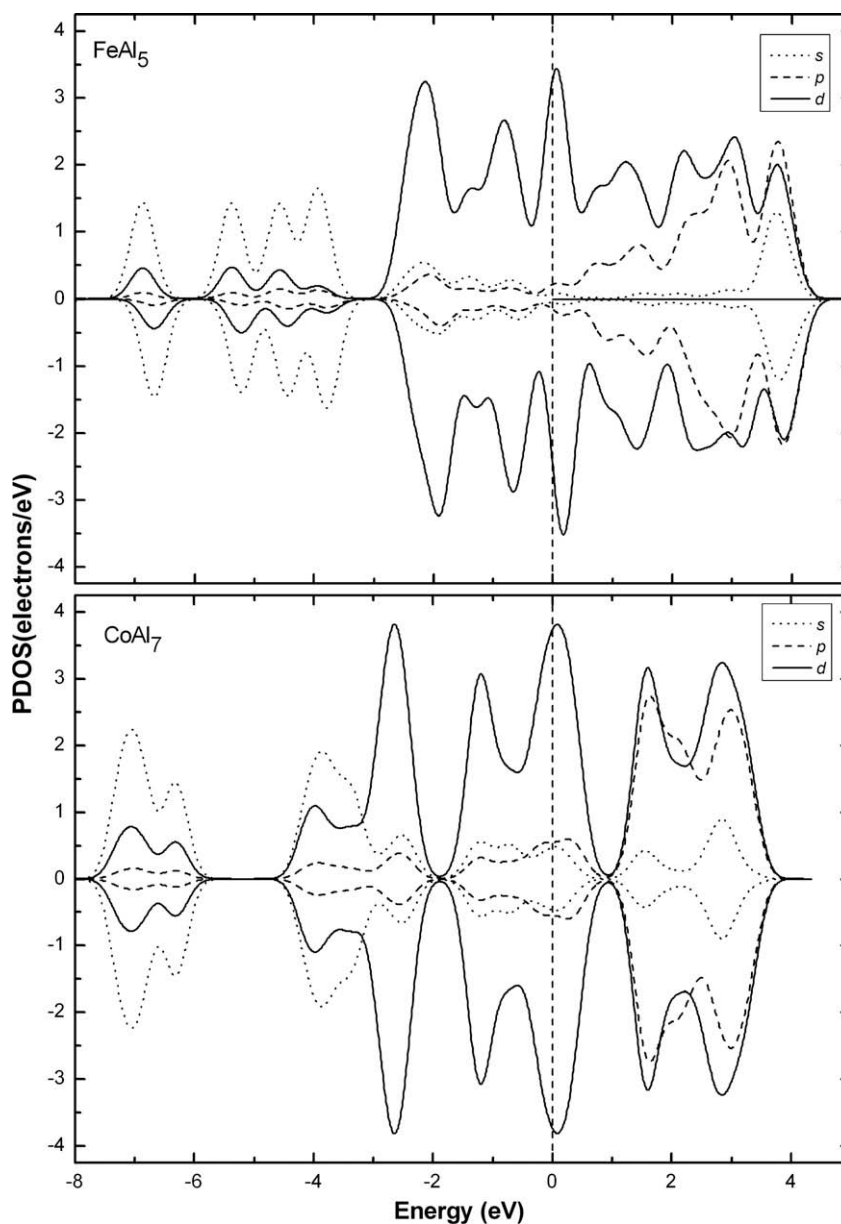


Fig. 5. The s -, p -, d -projected PDOS for the lowest-energy structures of FeAl_5 and CoAl_7 clusters. The dashed lines indicate the location of the HOMO level.

differences shows that MAI_3 clusters possess relatively higher stability. Besides, the analysis of the HOMO–LUMO gaps of MAI_n clusters indicates that MAI_{12} clusters have very small HOMO–LUMO gaps, and all the HOMO and LUMO states are non-degenerate and delocalized. Moreover, the result of NPA shows that the magnetism of the doped aluminum clusters is highly dependent on the 3d electrons of the transition metal dopant atoms. The relative orientation between the magnetic moments of the M atom and those of its neighboring Al atoms mainly exhibits an antiferromagnetic alignment for $CrAl_n$, $MnAl_n$, and $FeAl_n$, while it mainly shows a ferromagnetic alignment for $CoAl_n$ and $NiAl_n$ clusters.

Acknowledgments

The financial support from National Natural Science Foundation of China (Nos. 90306010 and 20371015), State Key Basic Research '973' Plan of China (No. 2007CB616911) and Program for New Century Excellent Talents in University of China (No. NCET-04-0653) is highly acknowledged.

References

- [1] C. Guet, P. Hobza, F. Spiegelman, F. David (Eds.), *Atomic Clusters and Nanoparticles*, NATO Advanced Study Institute, les Houches Session LXXIII, les Houches, 2000.
- [2] J.P. Connerade, A.V. Solov'yov (Eds.), *Latest Advances in Atomic Cluster Collisions: Fission, Fusion, Electron, Ion and Photon Impact*, Imperial College Press, London, 2004.
- [3] P.G. Reinhard, E. Suraud (Eds.), *Introduction to Cluster Dynamics*, Wiley-VCH, Weinheim, 2004.
- [4] F. Baletto, R. Ferrando, *Rev. Mod. Phys.* 77 (2005) 371.
- [5] M.B. Knickelbein, *Phys. Rev. Lett.* 86 (2001) 5255.
- [6] X.G. Gong, V. Kumar, *Phys. Rev. B* 50 (1994) 17701.
- [7] X. Li, L.S. Wang, *Phys. Rev. B* 65 (2002) 153404.
- [8] B.D. Leskiw, A.W. Castleman Jr., *Chem. Phys. Lett.* 316 (2000) 31.
- [9] B. Kiran et al., *Phys. Rev. Lett.* 98 (2008) 256802.
- [10] B.K. Rao, P. Jena, *J. Chem. Phys.* 111 (1999) 1890.
- [11] S.H. Yang, D.A. Drabold, J.B. Adams, A. Sachdev, *Phys. Rev. B* 47 (1993) 3.
- [12] W.D. Knight et al., *Phys. Rev. Lett.* 52 (1984) 2141.
- [13] M.Y. Chou, M.L. Cohen, *Phys. Lett. A* 113 (1986) 420.
- [14] Z.Y. Jiang, C.J. Yang, S.T. Li, *J. Chem. Phys.* 123 (2005) 204315.
- [15] S.F. Li, X.G. Gong, *Phys. Rev. B* 70 (2004) 075404.
- [16] J.J. Zhao et al., *Chem. Phys. Lett.* 443 (2007) 29.
- [17] A. Nakajima, T. Taguwa, K. Nakao, K. Hoshino, S. Iwata, K. Kaya, *J. Chem. Phys.* 102 (1995) 2.
- [18] S.K. Nayak, S.N. Khanna, P. Jena, *Phys. Rev. B* 57 (1998) 7.
- [19] V. Kumar, *Phys. Rev. B* 57 (1998) 15.
- [20] Q.L. Lu, A.F. Jalbout, Q.Q. Luo, J.G. Wan, G.H. Wang, *Chem. Phys.* 128 (2008) 224707.
- [21] X.G. Gong, V. Kumar, *Rev. Lett.* 70 (1993) 14.
- [22] B.V. Reddy, S.N. Khanna, S.C. Deevi, *Chem. Phys. Lett.* 333 (2001) 465.
- [23] M.S. Bailey, N.T. Wilson, C. Roberts, R.L. Johnston, *Eur. Phys. J. D* 25 (2003) 41.
- [24] G.S. Painter, C.L. Fu, F.W. Averill, *J. Appl. Phys.* 81 (1997) 5.
- [25] E.F. Rexer, J. Jellinek, E.B. Krissinel, E.K. Parks, S.J. Riley, *J. Chem. Phys.* 117 (2002) 82.
- [26] M. Calleja et al., *Phys. Rev. B* 60 (1999) 2020.
- [27] B. Delley, *J. Chem. Phys.* 92 (1990) 508;
B. Delley, *J. Chem. Phys.* 113 (2000) 7756 (DMOL is a density functional theory program distributed by Accelrys Inc.).
- [28] J.P. Perdew, *Electronic Structure of Solids'91*, in: P. Ziesche, H. Eschrig (Eds.), Springer, Berlin, 1991;
J.P. Perdew, J.A. Chevary, S.H. Vosko, K.A. Jackson, M.R. Pederson, D.J. Singh, C. Fiolhais, *Phys. Rev. B* 46 (1992) 6671.
- [29] P.J. Hay, W.R. Wadt, *J. Chem. Phys.* 82 (1985) 270;
W.R. Wadt, P.J. Hay, *J. Chem. Phys.* 82 (1985) 284;
P.J. Hay, W.R. Wadt, *J. Chem. Phys.* 82 (1985) 299.
- [30] M.J. Frisch et al., *GAUSSIAN 03*, Gaussian, Pittsburgh, PA, 2003.
- [31] B. Rosen, *Spectroscopic Data Relative to Diatomic Molecules*, Pergamon, Oxford, 1970.
- [32] M.B. Torres, E.M. Fernández, L.C. Balbás, *Phys. Rev. B* 71 (2005) 155412.
- [33] X. Liu, G.F. Zhao, L.J. Guo, Q. Jing, Y.H. Luo, *Phys. Rev. A* 75 (2007) 063201.
- [34] R.R. Zope, T. Baruah, *Phys. Rev. A* 64 (2001) 053202.
- [35] S.F. Li, X.G. Gong, *Phys. Rev. B* 74 (2006) 045432.